WATER CIRCULATION NEAR THE MIXED - WATER AND MICROBIOLOGIC ACTIVITY OF THE MESOZOIC DOLOMITE SEQUENCE, AN EXAMPLE FROM THE CENTRAL TAURUS, TURKEY

[1]Turhan Ayyildiz, [1]Erdogan Tekin, and [2]Muharrem Satir
[1]*Ankara University, Engineering Faculty, Department of Geological Engineering, 06100, Ankara - Turkey*
[2]*Eberhard Karls Universität Tübingen, Institut für Mineralogie, Petrologie und Geochemie, 72074, Tübingen, Germany*

ABSTRACT: Jurassic to Lower Cretaceous units, locating Central Taurus composed of thick dolomite with massive limestones beds and thinner dolomite beds with intercalated limestone are described. Various dolomite types include: Type I) dolomite formed as dolomicrite as mimetic replacement, Type II) dolosparite as a cloudy centre and clear rim in vugs, Type III) The planar-e texture dolomites are scattered in a micrite matrix, Type IV) Mottled dolomite present as zones of light colored dolomite crystals in a darker groundmass, Type V) Fracture and void filling dolomite (zoned dolomite, overgrowth and saddle dolomite). The investigated dolomites exhibit 0.1 to -2.0‰ PDB in $\delta^{18}O$ values relative to their $\delta^{13}C$ values (0.38 to 1.59‰ PDB) in the Middle Jurassic dolomites. The petrographic and isotopic characteristics support that dolomitization fluids were variable mixtures of fresh and marine waters related to changes in sea level. The late dolomitization phase was followed by diagenesis in the presence of meteoric fluids. During this period, calcite cements were precipitated within fractures. These calcites have characteristically low $\delta^{18}O$ and $\delta^{13}C$ values (-3.0 to -4.9 and -0.8 to -5.7‰ PDB, respectively).

Within the Jurassic dolostone facies, traces of bacterial activity were observed. The morphology of the Jurassic dolomite indicates that bacteria were involved in the formation of the dolomite. This bacterial activity is indicated by dolomite surfaces with knobby textures and bumpy structure.

Key words: Taurus Belt, Antalya, Hendos dolomite, biologic activity, isotopes

INTRODUCTION

The study area lies within the Central Taurus and comprises various carbonate rock units (Fig. 1).

Dolomite sequences ranging in thickness from 250 - 300 m are made up of typical examples of non-evaporitic platform dolostones of different age. To explain dolomite formation in non-evaporitic environments, many dolomitization models have been proposed (e.g., Friedman and Sanders 1967; Folk and Land 1975; Zenger and Dunham 1980; Hardie 1986). Microbial factors for dolomite precipitation were also described over the last century (Neher 1959; Folk 1993; Vasconcelos and Mckenzie 1997; Wright 1999; Gournay et al. 1999). In addition, the presence of former "bacterial" microspheres in ancient rocks has also been inferred from SEM (Scanning Electron Microscopy) examination (e.g. Folk 1993; Nielsen et al. 1997; Gournay et al. 1999). However, no detailed investigations of dolomite formation and bacterial activity about dolomite surface by SEM study have been reported for the area investigated here. The present study focuses on the microtextural properties and origin of dolomite beds of the Jurassic to the Lower Cretaceous. To help constraint its origin, dolomite samples have been analysed for stable isotope and trace element composition after petrographic and SEM characterisation. These data obtained were used to suggest a dolomitization model on the origin of the platform dolomite, related to fluid flow near the mixing zone.

GEOLOGICAL SETTING AND STRATIGRAPHY

The Jurassic to the Lower Cretaceous dolomite sequence is situated in the Central Taurus Belt, southern Turkey. The sequence consists of Jurassic to Middle Eocene units (Fig. 2). The Lower Jurassic sequence is predominated by reddish sandstone, conglomerate and mudstone with locally lignite and limestone - dolomite strata. The Middle Jurassic sequence has been divided into limestones and dolomites (Monod 1977). The Lower to Middle Jurassic limestone facies is made up of packstones-wackestones bearing spongia and macro fossil shells (brachiopod-echinoid), and mudstones. The Late Jurassic to Early Cretaceous (Berriasian) pelagic sequence consists of black marlstone and well-bedded black packstone with thin black chert layers (ammonites, Posidonia and Aulocomyella, fish remains and plant fragments are abundant), suggesting deposition in moderately deep water, in a protected and low-energy environment. The Early Cretaceous units mainly consists of limestone and dolomite interbeds. The Upper Cretaceous to Lower Eocene sequence is represented by bioclastic limestone (rudist) and nummulitic limestone. The Middle Eocene sequence is represented by clastics in flysch facies with volcanic strata.

Dolomite sequences generally exhibits two different bedding styles: (1) massive dolomites with numerous dolomite beds without interbedded limestone, which reach a maximum thickness of 200 m. These massive dolostone units occur at the Dogger-Malm boundary, and laterally change in thickness and pass to interbedded limestone; (2) stratal dolomite beds intercalated with limestone 1.5-2 m thick in the Early to Middle Jurassic and the Lower Cretaceous.

The Main Stratigraphic Gaps

Farinacci and Koyluoglu (1982) show that Bajocian (Dog-

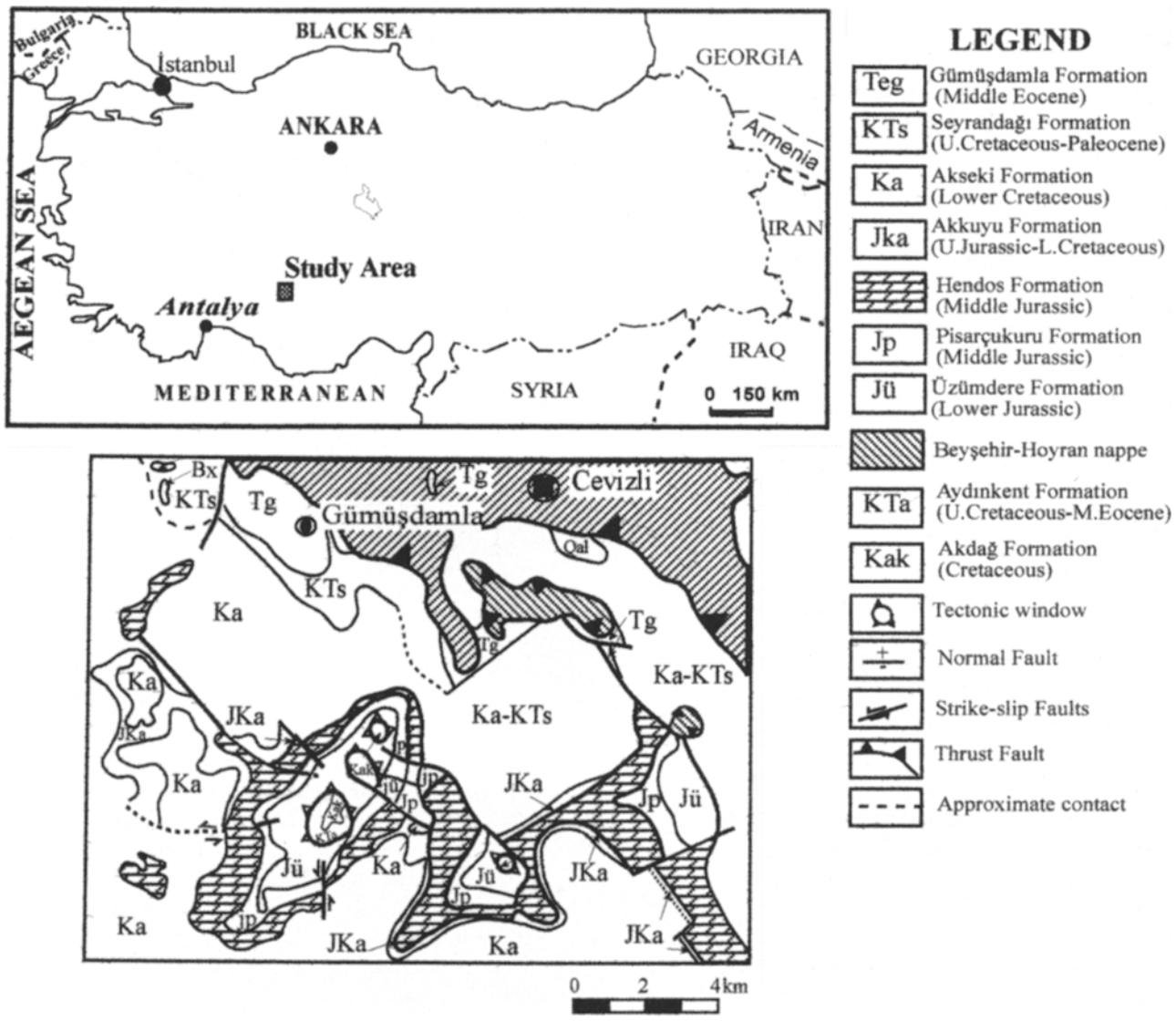

Figure 1. Location and simplified geologic map of the area of investigation (modified from Ayyildiz 1992).

ger) sediments are transgressive on Pliensbachian (Lias) strata. During the Cenomanian, there is bauxite occurs in lenses (e.g., Ozgul 1976, 1984; Monod 1977; Ozlu 1978; Ay-yildiz 1992) which suggest that a regional uplift of the platform above the sea level, due to the nappe emplacement. Detailed studies indicate that Coniacian, Santonian and perhaps part of the Campanian are missing (Farinacci and Koyluoglu 1982). The absence of deposition in the Lower and Middle Senonian is common all over the Taurus shelf.

METHODS

Petrographic investigations are based on examination of eighty polished thin sections using a polarizing optical microscope. Some of the thin sections were stained with Alizarin red-S. XRD (x-ray diffraction) analyses were carried out with a Rigaku Gelgerflex D / Max-Q / 2QWC model diffractometer. Microstructure properties and mineral identification were also determined in polished sections and by SEM (Scanning Electron Microscopy) and EDS (Energy Dispersive Analyses) with JSM 840 A and Tracor TN 5502 (Turkish Petroleum Coop., Research Centre) instruments, respectively. Quantitative geochemical analyses were performed using an Inductively Coupled Plasma Spectrometer (ICP) at ACME Laboratories in Canada. The stable isotope compositions were measured following the method of Longinelli and Craig (1967). Extracted CO_2 was measured on a Finnegun MAT 252 Mass Spectrometer. Data are reported in the conventional δ-notation in permil relative to PDB. Average analytical error is ± 0.1‰ for both C and O isotope analyses.

PETROGRAPHY

The paragenetic sequence includes various types of dolo-

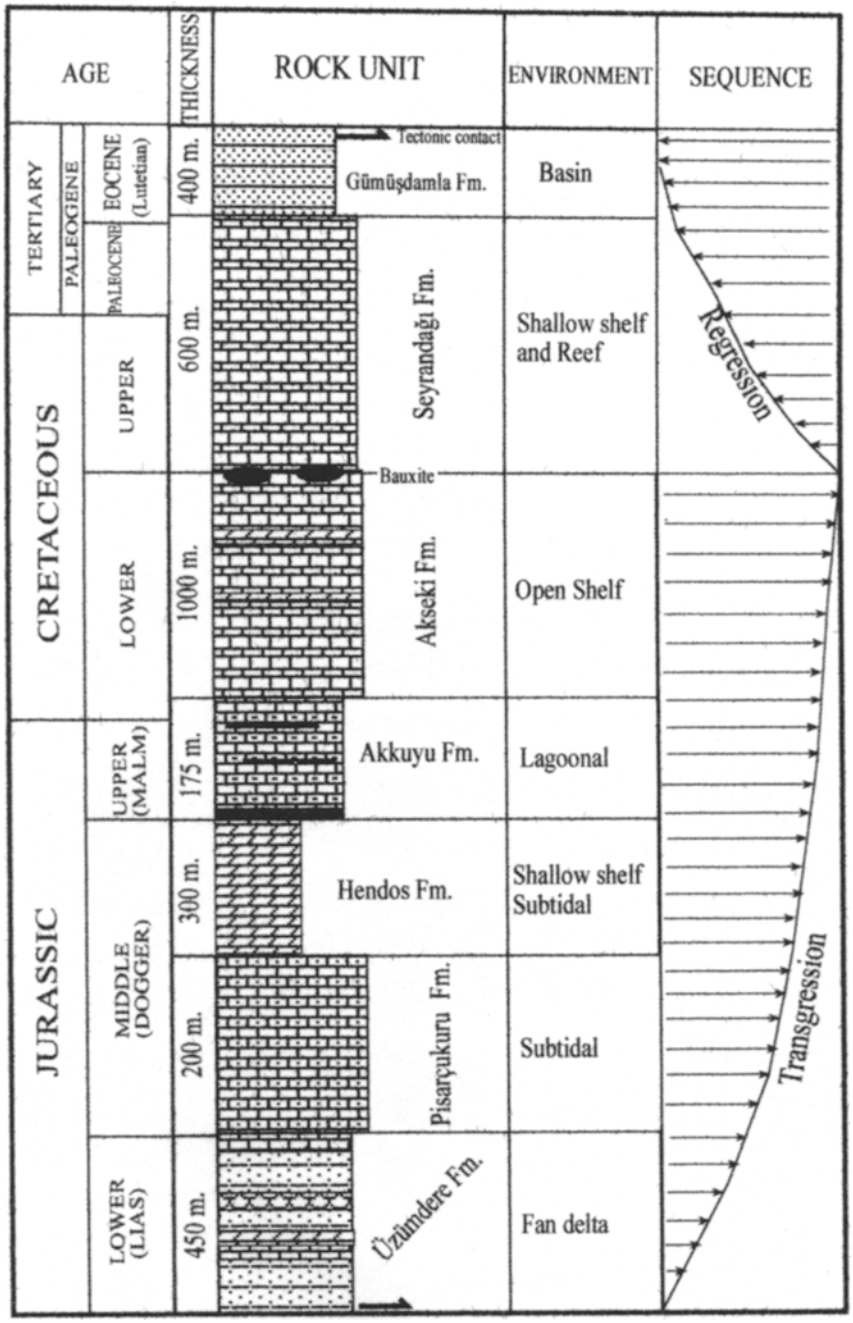

Figure 2. Columnar geological section of the investigated area (modified from Monod 1977).

mite and calcite. Sparite mosaic is the most abundant calcite type, whereas the most common dolomites are micritic. Some samples are observed as pure dolomicrite, with microvugs and fractures subsequently filled with dolomite and calcite. In addition, dolomites generally contain partly dolomitized micrite matrix. Dedolomitization is restricted to massive dolomite and partly dolomitized limestone.

The dolomite basic types, described as replacement and void filling dolomites, are divided into several subgroups such as micritic, mottled, overgrowth, and others. Dedolomite and calcite cement succeeded the varieties of the void-filling dolomites.

Replacive Dolomite

Type I.-- Generally homogeneous dolomicrite, but in some part, dolomitized allochems (such as fossil) can be visible which show mimetic replacement (Fig. 3a, b).

It has been suggested that this micritic dolomite was formed first (Varol and Magaritz 1992). However, SEM studies indicate that the dolomite crystal surface is composed of coalesced submicron-size bacterial traces and has a bumpy structure and knobby texture (Fig. 3c, d, e, f, g).

Type II.-- Dolosparite can be seen as a cloudy centre and

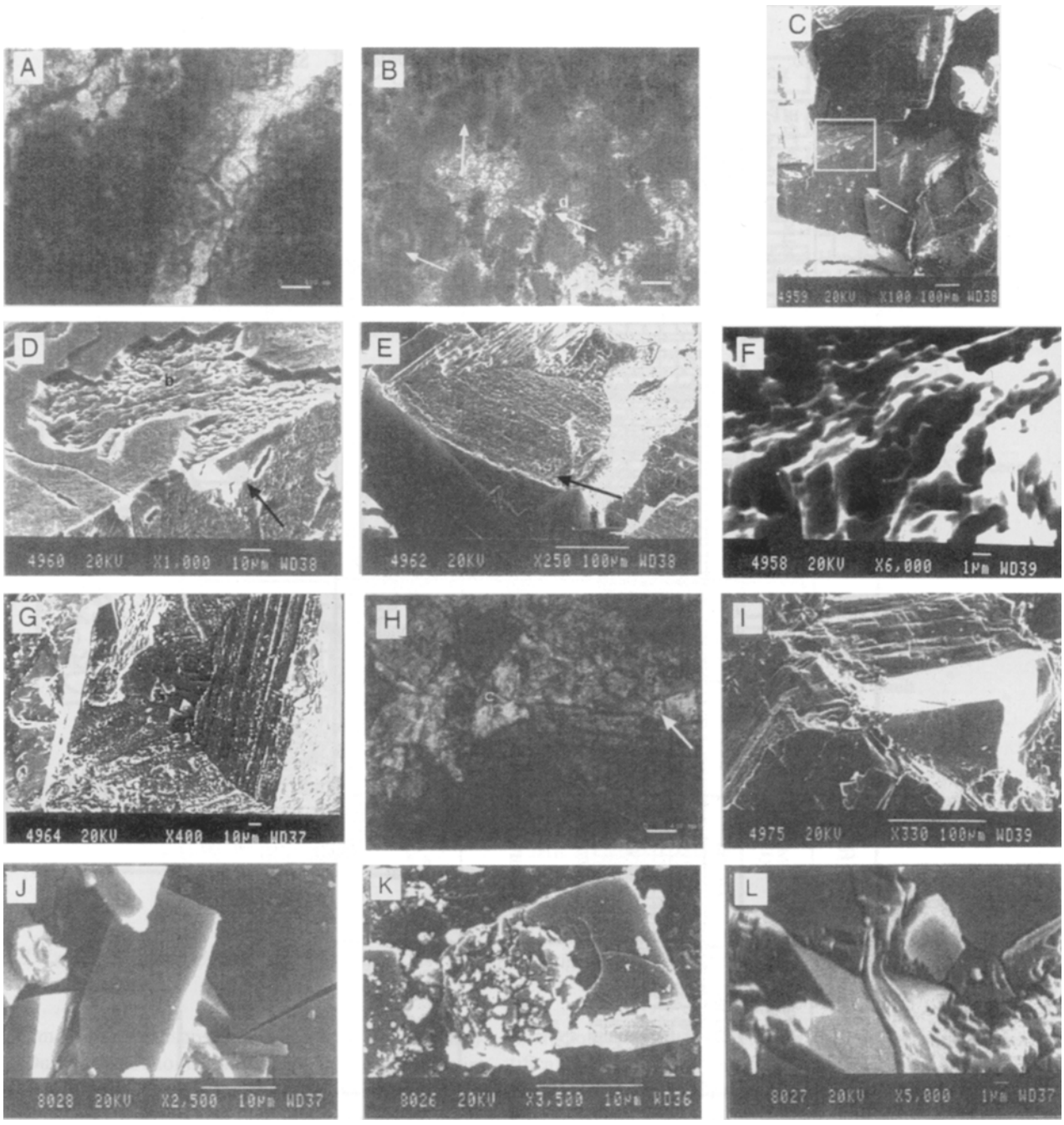

Figure 3. (A). Early stage dolomicrite occurrences, dissolution of the early dolomicrite with consequent development of related microfracture and precipitation of a clear dolomite rim around the dolomicrite nucleus. (B) Early dolomitization producing dolomicrite with some "ghosts" of fossils (arrow), dolosparite and dedolomitization (d). (C) SEM photomicrograph of bacterial activity traces on the dolomite surface. (D) SEM photomicrograph of coalesced submicron-size bacterial balls (spheroids) (b) and knobby texture on the dolomite surface (arrow). (E) SEM photomicrograph of a clear ream and moldic microporosity of the dolomite center. (F) SEM photomicrograph bacterial activity resulting in microboring and bumby structures of dolomite surfaces (G) SEM photomicrograph of patchy cloudy dolomite occurrences (H) Void-filling dolomite. Saddle crystals (arrow) within the fine crystalline dolomite most likely replaced the sparry calcite mosaic (c) within the fracture. (I) SEM photomicrograph of dolomite overgrowth, dark area is dolomicrite. (J) SEM photomicrograph of clear surface dolomite. (K) SEM photomicrograph of hollow dolomite rhombs. Corrosion of rhomb centers may indicate the onset of diagenetic "purification" of the dolomite section. (L) SEM photomicrograph of dolomite supersaturation and precipitated as jel.

clear rim, 15-20 microns in thickness. Generally cloudy dolosparite appears to be void-filling dolomite.

Most of the rhombs show clear zoning with a core and an outer zone. In some of rhombs, centres are cloudy and inclusion rich. In some cases, some ghosts of fossils (Fig. 3b) and ooids can be discerned within the dolomite mosaic.

Type III.-- The planer-e texture dolomites are scattered in a micrite matrix. The crystals are generally fine is size and represented by the clear crystals, however some micrite remained in central zones of dolomite rhombs.

Type IV.-- Mottled dolosparite is observed in the Jurassic dolomite.

This type of dolomite resulted from patchy dolomite replacement (Osmand 1956). The mottles are present as zones of light colored dolomite crystals in a darker groundmass, composed of subhedral and anhedral crystals.

Type V.-- Fracture and void-filling dolomite (Fig. 3a, h)

Fracture filling dolomite grains are coarse - grained, showing zoned growth structures. Petrographic observation shows that some vugs and fractures are lined by saddle dolomite crystals (Folk and Land 1975; Kaldi and Gidman 1982; Varol and Magaritz 1992; Miller and Folk 1994). Fracture spaces are not only filled by this type of dolomites but also filled by coarse calcite crystals. Saddle dolomite cement is precipitated in fracture walls as shown in Fig. 3h. The curved crystals exhibit very undulose extinction, and grow towards vug centres. SEM studies show that this zone overgrows dolomite rhombs (Fig. 3i). Overgrowth represents only an outer overgrowth on existing rhombs (micritic dolomite) and is considered to be a replacement dolomite. These dolomite types consist of clear dolomite and none display evidence for bacterial activity. Due to this overgrowth, crystals of 100-120 μm were produced. Volumetrically, overgrowth dolomite is insignificant relative to dolomite.

Dedolomite

Dedolomite occurrence are observed in two types early and late diagenesis. The early diagenetic type was observed in partly dolomitized limestone facies. Generally, the micritic dolomite centre has changed to dedolomite, whereas the outer light zone is still dolomite (Fig. 3b). The late diagenetic dedolomite is commonly formed in fractures and/or on the zoned dolomite. Generally, dedolomitization is observed with the cementing saddle dolomite crystals.

Coarse calcite cements occur towards the micro-fractures or vug centre as the last cement filling (Fig. 3h, i) the remaining pore space. The second phase of calcite is observed in discrete zones of the dolomite rhombs, consistently at the boundary of core and outer zone. The thin calcite zones within these dolomites have a bright colour. This zone is considered to have formed after the dolomite rhombs by selective dissolution of one of the inner zones of the dolomite rhombs. Calcite precipitation followed the dissolution gaps.

Interpretation

Several features that indicate subareal exposure and alteration in the presence of meteoric water include: 1) karst and unconformities boundary; 2) secondary pores filled by later mixed water solution; and 3) bauxite lenses as upper boundary of the Early Cretaceous.

In the Jurassic-Cretaceous dolomite, two main dolomite types include micritic and coarse dolomite (Type I and II) crystals. Type IV, mottled dolomite, occurs as fabric selectively, resulting from inhomogeneties in the original limestone texture. Zoned dolomite is observed especially in fracture and vugy fillings (Type V). The Jurassic dolomites have abundant micropores and bumpy crystal surfaces. Chafets and Folk (1984) suggest that spherical bacterium, filaments and organic tissues from other primitive organisms readily decay, leaving moldic microporosity. This could explain how the micropores were established. In the Bahamas, the base of the modern freshwater-seawater mixing zone is anaerobic and bacterially mediated sulphate reduction, driven by the oxidation of organic matter, has been demonstrated to be an important geochemical process (Smart et al. 1988; Stoessell 1992; Bottrell et al. 1993). In the study area, the Upper Jurassic to Lower Cretaceous (Berriasian) deposition occurred in a basinal environment surrounded by a carbonate platform and includes "black band" at its base. The organic matter was particularly well preserved in anoxic, perhaps even euxinic, bottom conditions during deposition. These data are supported by $\delta^{13}C$ values (Baudin et al. 1999). Organic matter gets used up during sulphate reduction. Probably, the bacteria bearing water percolated towards lower part and used the dolomite (Fig. 4). As a result of this bacterial activity, dolomite surfaces appear to be submicron - sized spheroids. In addition, Ayyildiz et al. (2001) suggested that Cyanobacteria and Endolithic algae are thought to have contributed to the formation of the Middle Jurassic oolite. These data indicate that bacterial activity in the micro - environment was important during the Middle Jurassic. However, the Lower Cretaceous dolomites have clear surfaces with planar crystals (Sibley and Gregg 1987) and no traces of bacteria (Fig. 3j). Probably, there was no suitable micro or macro environment for bacteria during the Lower Cretaceous time.

Some of dolomite crystals display distinctive cloudy centers surrounded by clear limpid rims. Sibley (1980) suggested that this was a result of pore fluid evolution from a state of under saturation as growth continues in the mixing zone. In addition, regular compositional zoning may sug-

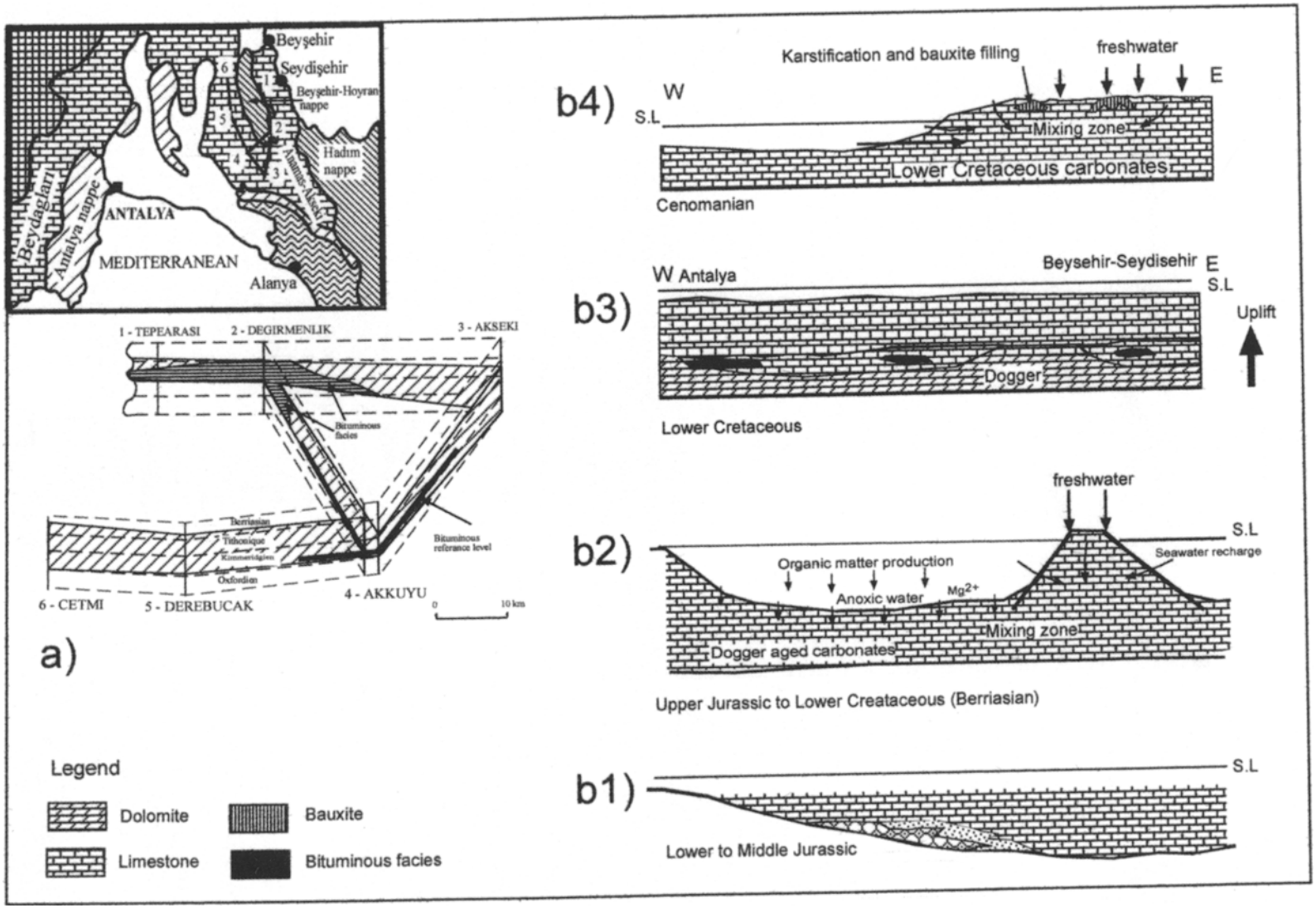

Figure 4. (a) Variations of the Akkuyu Formation facies (modified from Monod 1977). (b1) Schematic illustration of the carbonate precipitation during the Lower to Middle Jurassic time. (b2) Schematic of dolomitization fluids were variable mixtures of marine waters and fresh waters related to changes in sea level and microbiologic activity during the upper Jurassic time. (b3)After the Lower Cretaceous carbonate overlie the Jurassic sequence, eastern and northeastern part of the platform uplift since the Beysehir Hoyran nappe, emplacement from northeastern. (b4) During the Cenomanian, the Lower Cretaceous carbonates were intensely karstified to be related to the lowering of relative sea level and dolomitization was caused by mixing zone.

gests that fluid chemical composition fluctuated during the precipitation of zoned dolomite. Zoned dolomite cements formed in the mixing zone of the Yucatan Peninsula (Ward and Halley 1985) and of the Florida aquifer (Randazzo and Cook 1987). Varol and Magaritz (1992) suggested that precipitation of clear dolomite rims around the dolomicrite nucleus and precipitation of sparry calcite cement followed initial dissolution of the early dolomicrite. However, experimental studies show that dolomite dissolution is considerably slower than calcite dissolution, particularly at low temperature (Busenberg and Plummer 1982). Gregg and Sibley (1984) state that non planar crystal textures may indicate elevated temperatures (>50°C). Low Sr^{2+} content of dolostone and dolomites associated with freshwater calcite indicate that dolomitizing fluid was hyposaline rather than hypersaline (Matsumoto et al. 1988). These data indicate that probably some of the undolomitized micrite and bioclasts were dissolved by meteoric fluids, and pore-filling dolomite precipitated. Unstable biogenic carbonate dissolution probably followed the formation of zoned dolomites. Mimetic replacement is the main texture indicating that slow dolomitization processes are dominant.

Saddle crystals was precipitated in some cavities and fractures, and closely resemble the karstic dolomite described by Buchbinder et al. (1984). Saddle crystals also show dissolution and late dedolomitization indicating that dolomite was the least stable, probably a replacement by rapidly precipitated calcian phase. Some dolomite cores and rims were partly dissolved as hollow textures, interpreted to result from the dissolution of Ca-rich dolomite (Fig. 3k). In addition, fracture - filling dolomite was changed to calcite but keeping the original crystal shapes, interpreted as meteoric waters influx after dolomite cement formation. The latest diagenetic event of the calcite cement precipitation may have originated from meteoric fluids. There is evidence for the supersaturation and precipitation as jelly (Fig. 3 l). Probably, when the lowering of the relative sea level continued during Senomanian times, and followed by fresh water input. As a result of water chemistry changing, supersaturation may have taken place.

GEOCHEMISTRY

Major - Minor Element Geochemistry

The Jurassic-Cretaceous dolomite has MgO concentrations from 18.38 to 19.80%, and from 30.25 to 36.77 weight % CaO as determined by ICP analysis. Sr^{2+} concentration ranges from 61 to 141 ppm, Fe^{2+} values are 35.9 and 107.9 ppm for Dogger - L. Cretaceous dolomite, and the L.

Jurassic dolomite value is 668.6 ppm. Mn^{2+} is only detectable in the Lower Jurassic dolomite (23.2 ppm), the other dolomites have very low Mn concentrations (<7.7 ppm). Na^{+} values are between < 7.4 and 22. 2 ppm. Sr^{2+} contents of the limestones are between 45.8 and 326.2 ppm.

Stable Isotopes

Stable isotope compositions from the Middle Jurassic dolomites have values of -1.97 to +1.72‰ for $\delta^{18}O$, and +0.38 to +1.59‰ for $\delta^{13}C$ (Fig. 5). The oxygen and carbon isotope compositions of the calcites are -3.22‰ and -4.94‰, and -3.97‰ and -5.67‰ , respectively. Furthermore, the stable isotope compositions of the Lower Cretaceous dolomite and the calcite have been analysed. Oxygen isotope value of the Lower Cretaceous dolomite -0.69‰, whereas carbon value +1.45‰. The $\delta^{18}O$ composition of the calcite is -3.03‰ and carbon value is -0.78‰.

Interpretation

The concentration of Sr^{2+} in the dolomite is relatively low (between 61 and 141 ppm), similar to that of other ancient dolomites (e.g. Mattes and Mountjoy 1980; Wallace 1990). Furthermore, waters must have had Sr/Ca ratio as low as or even lower than that of seawater to cause Sr concentrations less than 100 ppm. Fe^{2+} and Mn^{2+} concentration is also very low, except for the Lower Jurassic dolomite support their formation in an oxidising. Na^{+} levels are relatively high for marine dolomites, however; low Na levels of the dolomites of this study may indicate mixing zone dolomites (Warren 2000). Na^{+}, Al^{2+}, K^{+} and Fe^{2+} concentration are positively correlated with silica content in the Liassic dolomite, indicating contamination of these elements by detrital siliciclastic silt and sand, and possibly clays.

Isotopic data on dolomites is plotted together with published data in Fig. 6. Isotopic data of the dolomites fall in the mixing zone defined by Choquette and Steinen (1980). Oxygen isotopic compositions fall in a narrow range from

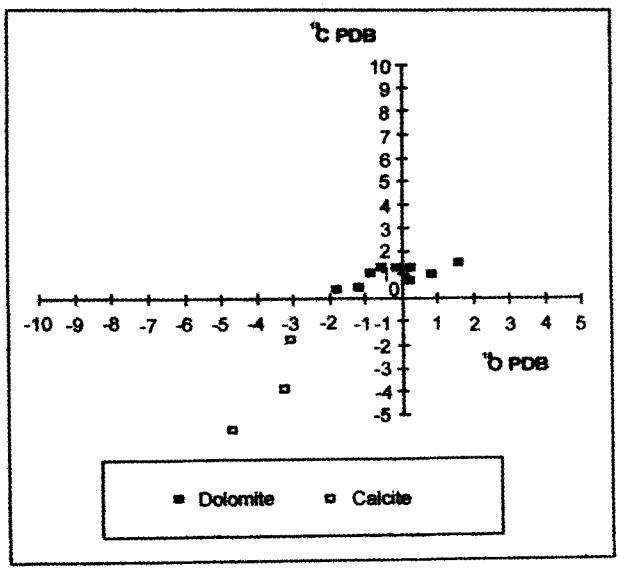

Figure 5. Cross-plot of oxygen and carbon isotope compositions from the Lower Middle Jurassic and Lower Cretaceous dolomites.

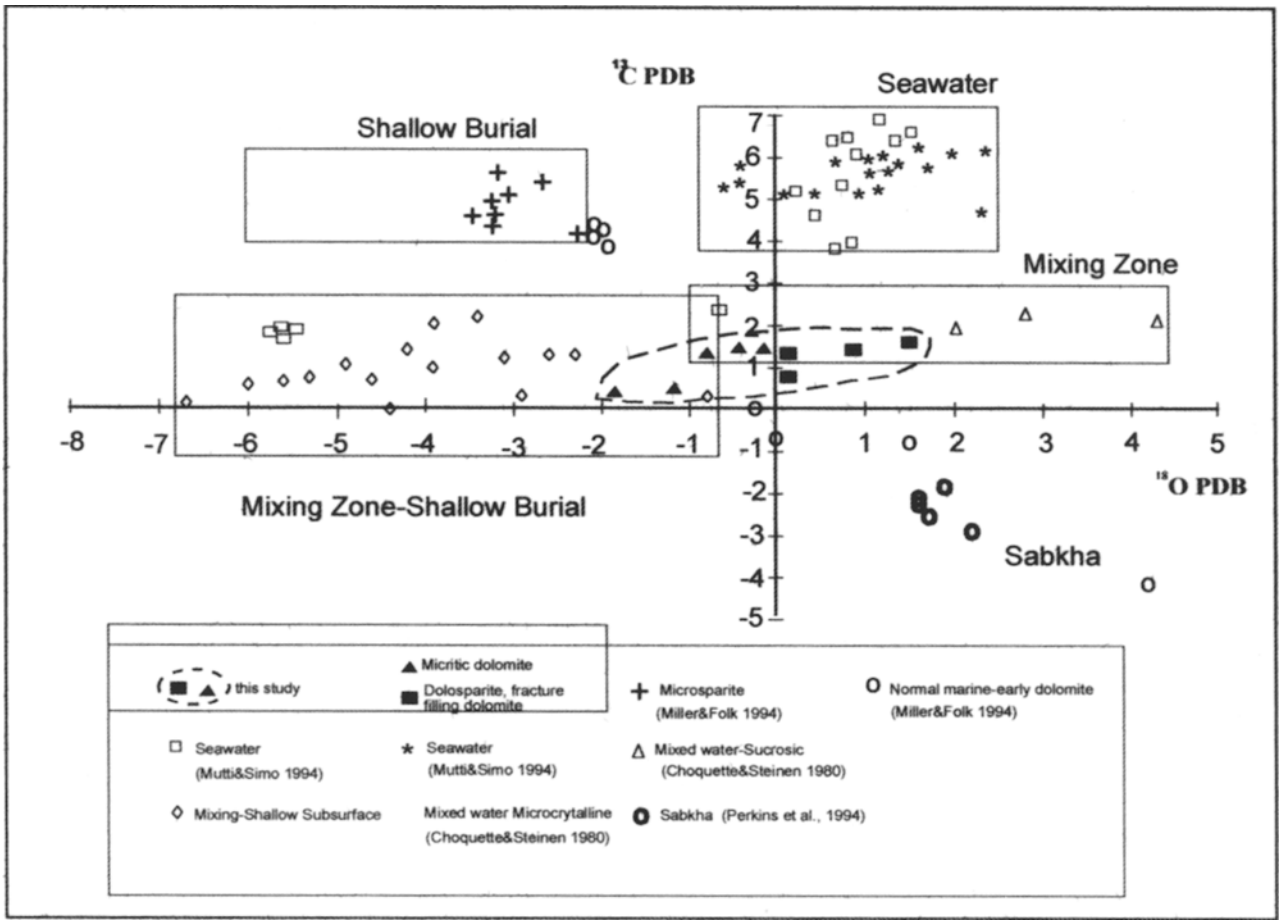

Figure 6. Comparison of isotopic data of the Lower- Middle Jurassic and the Lower Cretaceous dolomites with those from other dolomites elsewhere.

1.72‰ to -1.97‰ for all types of dolomite and there is not a correlation between the isotopic record and age or petrographic type. Dolomite formed in evaporitic and normal marine settings displays positive $\delta^{18}O$ values. However, the negative values now displayed by the zoned and clear dolomites suggest that they have recrystallised with the adoption of the negative $\delta^{18}O$ signature (Fig. 6). Hence, it can be deduced that dolomites with low Sr^{2+} concentration and negative $\delta^{18}O$ values were probably formed in the presence of low-salinity meteoric waters. However, positive isotopic data (micritic and mottled dolomite) also support a marine derived fluid. Carbon isotopic compositions range between +0.38 $\delta^{13}C$‰ and 1.59‰ PDB (Fig. 5). $\delta^{13}C$ values between 0 and +4‰ are typically marine signatures, confirming marine origin of the carbonates (Tucker and Wright 1990). We suggest that micritic and the core of the zoned dolomite, formed in marine waters while clear dolomite and zone of the rim, precipitated in mixed water.

The calcite $\delta^{18}O$ isotopic values (-3.03 to -4.94‰ PDB) are depleted by around 3‰ in ^{18}O compared to those of dolomites (1.72 to -1.97‰ PDB). These data indicate that calcite cement in the pore space formed in the presence of meteoric water or from marine waters at elevated temperatures. However, according to Land (1980, 1985) dolomite formed under the same conditions as calcite, should be enriched in ^{18}O by about 3‰. As this is the case, it would support that dolomite also formed in the presence of or was subsequently altered by meteoric water bearing fluids. The negative $\delta^{13}C$ values of the studied calcites (-0.78 to -5.67‰ PDB) argue for a large input of carbon depleted in ^{13}C derived from the decay of organic material.

TIMING OF DOLOMITIZATION

The different petrographic fabrics in the central Taurus dolostone (Jurassic to Cretaceous) indicate several stages of dolomitization. Considering the hypothesis, dolomitization at the Middle Jurassic limestones probably occurred after during the Upper Jurassic time. The first dolomitization occurred due to seawater circulating near the mixing zone during the Late Jurassic. The Upper Jurassic to Lower Cretaceous (Berriasian) carbonates include pelagic limestones and a peculiar 'black band' at its base. Baudin et al. (1999) stated that deposition in moderately deep water, in a protected and low-energy environment with restricted bottom circulation, at least during 'black band' deposition during the Upper Jurassic. Wide variations in the texture, min-

eralogy, and chemistry of this unit can be explained as the result of the eustatic sea-level change, and both differential uplift and subsidence of each locality relative to hydrological zones. When relative sea level continued to drop, either through additional uplift, the dolomitizing mixing zone migrated downward through the Middle Jurassic limestones (Fig. 4b2). Zoned dolomites at the Middle Jurassic dolomites were repeatedly exposed to freshwater and mixing zones during this stage. This can be explained through fluctuations in the vertical movement of the limestones or eustatic sea-level change. The role of microbial activity, and in particular the importance of sulfate-reducing bacteria, is difficult to evaluate for the dolomites in this study. Because the negative $\delta^{13}C$ value of the dolomite cement indicate that microbial degradation of organic matter was significant. However, the $\delta^{13}C$ values are not as negative as mixed-water dolomites from Lagoa (Vasconcelos and Mckenzie 1997) or marine dolomites from the sulphate-reduction zone (Mazzullo 1999). The presence of both hopane-rich and sulphur-rich nanoscopically amorphous organic matters may be the result of strong sulphate-reducing bacterial activity during the Upper Jurassic time (Baudin et al. 1999). Sulphate-reducing bacteria saturated with water may continue through the mixing-zone (Fig. 4b2). The loading of sulphate reducing bacteria might be provides an ideal substrate for bacteriological processes. This stage was followed by subsidence over the Jurassic carbonates and/or sea-level rise due to eustatic effects (Fig. 4b3). After limestones at the Lower Cretaceous were deposited, eastern and northeastern part of the study area was uplift since allocthonous unit emplacement over the carbonate platform (Ozgul 1976). Due to the uplift during the Cenomanian, the top of the Lower Cretaceous limestones were subjected to karstification and karst pockets are filled with bauxite (e.g., Ozgul 1976; Monod 1977; Ozlu 1978). The limestones at the Lower Cretaceous remaining in mixing zone dolomitization (Fig. 4 b4). The negative $\delta^{18}O$ isotope value (- 0.69‰ PDB) support mixing zone dolomitization. The calcite cement after dolomite formation seems to have been formed in the latest diagenetic stage of the Central Taurus Mesozoic dolostone.

CONCLUSIONS

The Jurassic to Cretaceous carbonates of this study occurred in a carbonate platform without evaporite mineral association. Different types of dolomite and calcite facies were formed during early and late diagenetic stages related to sea level variations. Low Sr^{+2} concentrations and $\delta^{13}C$ and $\delta^{18}O$ values and petrographic evidence support a late dissolution of dolomite within a mixing-zone between seawater and meteoric water. The presence of an unconformity on the top of the Lower Cretaceous formations shows that flushing by meteoric waters can be related to a major relative fall in sea - level in the study area. Generally, saddle crystal and fracture-filling types of dolomites were developed in the presence of meteoric water. Depletion $\delta^{18}O$ values of the calcite cement support that the precipitation of the calcite from meteoric water is also common in the fractures. In addition, bacterial activity traces on the Jurassic dolomite crystal surface were recognised. Probably bacteria and other microbes played an essential role in dolomite of the Late Jurassic to the Early Cretaceous (Berriasian) sediments. Absence of bacterial activity for dolomites of the Early Cretaceous indicate that bacterial activity was not important during this time.

In conclusion, we suggest that the major part of dolomite formed due to the seawater circulation and induced by mixing zone. After dolomite formation within mixing-zone, probably as a result of bacterial activity is thought to have been the most important factor by dolomite surfaces with knobby textures and bumpy structure in the Middle Jurassic platform dolomites.

ACKNOWLEDGMENTS

We thank Dr. Torsten Venuemann (Tübingen University, Germany) for a critical reading of the manuscript, which improved the paper.

REFERENCES

AYYILDIZ, T., 1992, Üzümdere - Akkuyu (Akseki-Antalya) civarinin petrol olanaklari, Ms Thesis, Ankara University, 198 p., unpublished (in Turkish).

AYYILDIZ, T., TEKIN, E., and FRIEDMAN, G.M., 2001, Microtextural properties of ooids in the Middle Jurassic-Lower Cretaceous, central Taurus carbonate platform, Antalya, Turkey: *Carbonates and Evaporites,* v. 16, p. 1-7.

BAUDIN, F., TRIBOVILLARD, N., LAGGOUN-D FARGE, F., LICHTFOUSES, E., MONOD, O., and GARDIN, S., 1999, Depositional environment of a Kimmeridgian carbonate 'black band'(Akkuyu Formation), south-western Turkey: *Sedimentology*, v. 46, p. 589-602.

BOTTRELL, S.H., CAREW, J.L., and MYLROIE, J.E., 1993, Bacterial sulphate reduction in flank margin environments: Evidence from sulphur isotopes. *In* B. White, ed., Proceedings of the sixth symposium on the geology of the Bahamas. Bahamian Field Station. San Salvador Island, Bahamas, p. 17-21.

BUCHBINDER, L.G., MAGARITZ, M., and GOLDBERG, M., 1984, Stable isotope study of karstic-related dolomitization. Jurassic rocks from the coastal plain, Israel: *Journal of Sedimentary Petrology*, v. 54, p. 236-257.

BUSENBERG, E. and PLUMMER, L.N., 1982, The kinetics of dissolution of dolomite in CO_2 - H_2O systems at 1.5 to 65°C and 0 to 1 atm PCO_2: *American Journal of Science,* v. 282, p. 45-78.

CHAFETZ, H.S. and FOLK, R.L., 1984, Travertines: Depositional morphology and the bacterially constructed constituents: *Journal of Sedimentary Petrology*, v. 54, p. 289-316.

CHOQUETTE, P.W. and STEINEN, R.P., 1980, Mississipian non-supratidal dolomite, Ste. Genevieve limestone, Illinois Basin: evidence for mixed-water dolomitization, *in* D.H. Zenger, J.B. Dunham, and R.L. Ethington, eds., Concepts and models of dolomitization. SEPM. Spec. Publ. v. 28, p. 163-196.

FARINACCI, A. and KOYLUOGLU, M., 1982, Evolution of the Jurassic Cretaceous Taurus shelf (Southern Turkey): *Bollettino della Soc. Paleont. Italiana*, v. 21, p. 267-276.

FOLK, R.L. and LAND, L.S., 1975, Mg/Ca ration and salinity. Two controls over crystallization of dolomite: *AAPG Bulletin*, v. 59, p. 60-68.

FOLK, R.L., 1993, SEM imaging of bacteria and nannobacteria in carbonate sediments and rocks: *Journal of Sedimentary Petrology*, v. 63, p. 990-999.

FRIEDMAN, G.M. and SANDERS, J.E., 1967, Origin and occurrence of dolostone. *In* G.V. Chilinger, H.J., Bissell, and Rhodes Fairbridge, eds., Developments in Sedimentology. Elsevier Publishing Company, no. 9A, p. 269-348.

GOURNAY, J.P., KIRKLAND, B.L., FOLK., R.L., and LYNCH, F.L., 1999, Nanometer-scale features in dolomite from Pennsylvanian rocks, Paradox Basin, Utah: *Sedimentary Geology*, v. 126, p. 243-252.

GREGG, J.M. and SIBLEY, K.L., 1984, Epigenetic dolomitization the origin of xenotopic dolomite texture: *Journal of Sedimentary Petrology*, v. 54, p. 907-931.

HARDIE, L.A., 1986, Dolomitization. A critical view of some current views repectives: *Journal of Sedimentary Petrology,* v. 57, p. 166-183.

KALDI, J. and GIDMAN, J., 1982, Early diagenetic dolomite cements: examples from the Permian Lower Magnesian Limestone of England and Pleistocene carbonates of the Bahamas: *Journal of Sedimentary Petrology*, v. 52, p. 1073-1085.

LAND, L.S., 1980, The isotopic and trace element geochemistry of dolomite: the state of the earth. Concepts and Models of Dolomitization, *in* D.H. Zenger, J.B. Dunham, and R.L. Ethington, eds., SEPM Special Publication, no. 28, p. 87-110.

LAND, L.S., 1985, The origin of massive dolomite: *Journal of Geologial Education*, v. 33, p. 112-125.

LONGINELLI, A. and CRAIG, H.,1967, Oxygen-18 variations in sulfate and carbonate ions in sea-water and saline lakes: *Science*, v. 156, p. 1431-1438.

MATSUMATO, R., LIJIMA, A. and KATAYAMA, T., 1988, Mixed water hydrothermal dolomitization of the Pliocene Shihara Limestone, Izu Peninsula, Central Japan: *Sedimentology*, v. 35, p. 979-999.

MATTES, D.H. and MOUNTJOY, E.W.,1980, Burial dolomitization of the Upper Devonian Miette buildup, Jasper National Park, Alberta, *in* D.H. Zenger, J.B. Dunham, and R.L. Ethington, eds., Concepts and models of dolomitization. SEPM Special Publication, no. 28, p. 259-297.

MAZZULLO, S.J., 1999, Organogenic dolomitization in peritidal to deep-sea sediments: *Journal of Sedimentary Research*, v. 70, p. 10-23.

MILLER, J.K. and FOLK, R.L.,1994, Petrographic, geochemical and structural constraints on the timing and distribution of postlithification dolomite in the Rhaetian Portoro ('Calcar Nero') of the Portovenere Area, La Spezia, Italy, *in* B.H. Purser, M.E. Tucker, and D.H. Zenger, eds., Dolomites: A volume in honour of Dolomieu. International Association of Sedimentologists, Special Publication, no. 21, p. 187-202.

MONOD, O., 1977, Recharches geologiques dane les Taurus occidental au sud de Beysehir, These Eresente a I' Universite de Paris sud Centre d' Orsay, 442 p.

MUTTI, M. and SIMO, J.A.,1994, Distribution, petrography and geochemistry of early dolomite in cyclic shelf facies, Yates Formation (Guadalupian), Capitan Reef Complex, USA, *in* B.H. Purser, M.E. Tucker, and D.H. Zenger, eds., Dolomites: A volume in honour of Dolomieu. International Association of Sedimentologists, Special Publication, no. 21, p. 91-109.

NEHER, J., 1959, Bakterien in tieferliegenden Gesteinslagen: *Eclog. Geol. Helv.*, v. 52, p. 619-625.

NIELSEN, P., SWENNEN, R., DICKSON, J.A.D., FALLICK, A.E., and KEPPENS, E., 1997, Spheroidal dolomites in a Visean karst system bacterial induced origin: *Sedimentology*, v. 44, p. 177-195.

OSMAND, J.C., 1956, Mottled carbonate rocks in the Middle Devonian of eastern Neveda: *Journal of Sedimentary Petrology*, v. 26, p. 32-41.

OZGUL, N., 1976, Toroslarin bazi temel jeoloji özellikleri: *TJK Bulteni*,. v. 19, p. 65-78 (in Turkish).

OZGUL, N., 1984, Stratigraphy and tectonic evolution of the Central Taurides. *In* O. Tekeli and C. Gönciuoğlu, eds., Geology of the Taurus Belt, p. 11-26.

OZLU, N., 1978, Akseki - Seydisehir boksitlerinin kökeni hakk nda yeni bulgular: *TJK Bulteni*, v. 22, p. 215-227 (in Turkish).

PERKINS, R.D., DWYER, G.S., ROSOFF, D.B., FULLER, J., BAKER, P.A. and LLOYD, R.,1994, Salina sedimentation and diagenesis: West Caicos Island, British West Indies, *in* B.H. Purser, M.E. Tucker, and D.H. Zenger, eds., Dolomites: A volume in honour of Dolomieu. International Association of Sedimentologists, Special Publication, no. 21, p. 37-54.

RANDAZZO, A.F. and COOK, D.J., 1987, Characterization of dolomitic rocks from the coastal mixing zone of the Floridan aquifer: *Sedimentary Geology*, v. 54, p. 169-192.

SIBLEY, D.F., 1980, Climatic control of dolomitization, Seroe Domi Formation (Pliocene). N.A. Bonarie, *In* Zenger, D.H., Dunham, J.B. and Ethington, R.L., eds., Concepts and models of dolomitization. SEPM Special Publication, v. 28, p. 247-258.

SIBLEY, D.F. and GREGG, J.M., 1987, Classification of dolomite rock textures: *Journal of Sedimentary Petrology*, v. 57, p. 967-975.

SMART, P.L. DAWANS, J.M. and WHITAKER, F., 1988, Carbonate dissolution in a modern mixing zone: *Nature*, v. 335, p.811-813.

STOESSELL, R.K., 1992, Effect of sulfate reduction on $CaCO_3$ dissolution and precipitation in mixing-zone fluids: *Journal of Sedimentary Petrology,* v. 62, p. 873-880.

TUCKER, M.E. and WRIGHT, V.P., 1990, Carbonate sedimentology. Blackwell Science, Oxford, p. 278-279.

VAROL, B. and MAGARITZ, M., 1992, Dolomitization, time boundaries and unconformities: examples from the dolostone of the Taurus Mesozoic sequence, south-central Turkey: *Sedimentary Geology*, v. 76, p. 117-133.

VASCONCELOS, C. and MCKENZIE, J.A., 1997, Microbial mediation of modern dolomite precipitation and diagenesis under anoxic conditions (Lagoa Vermelha, Rio de Janerio, Brazil): *Journal of Sedimentary Petrology*, v. 67, p. 378-390.

WALLACE, M.W., 1990, Origin of dolomitization on the Barbwire Terrace, Canning Basin. Western Australia: *Sedimentology,* v. 37, p. 105-122.

WARD, W.C. and HALLEY, R.B., 1985, Dolomitization in a mixing zone of near seawater composition, late Pleistocene, north-eastern Yucatan Peninsula: *Journal of Sedimentary Petrology*, v. 55, p. 407-420.

WARREN, J., 2000, Dolomite: occurrence, evolution and economically important Associations: *Earth-Science Reviews*, v. 52, p. 1-81.

WRIGHT, D.T., 1999, The role of sulphate-reducing bacteria and cyanobacteria in dolomite formation in distal ephemeral lakes of the Coorong region, South Australia: *Sedimentary Geology*, v. 126, p. 147-157.

ZENGER, D.H. and DUNHAM, J.B., 1980, Concepts of models of dolomitization an Introduction: SEPM Special Publication, v. 28, p. 1-19.